Soft Matter

RSC Publishing

PAPER

View Article Online
View Journal

Published on 07 October 2013. Downloaded by National Tsing Hua University on 07/11/2013 14:17:47.

# Packing DNA with disc-shaped bicelles†

Cite this: DOI: 10.1039/c3sm51703a

Po-Wei Yang,[a] Tsang-Lang Lin,*[a] Tsung-Yi Lin,[a] Ching-Hsun Yang,[a] Yuan Hu[a] and U-Ser Jeng[b]

Cationic lipid–DNA (CL–DNA) complexes can be used as non-viral vectors to improve transfection efficiency in gene therapy. It is greatly desirable to develop new ways of packing DNA in order to make breakthroughs on the development of highly efficient DNA delivery systems. Different from the widely-studied vesicle based CL–DNA complexes, we have developed a novel cationic bicelle–DNA complex system by mixing cationic bicelles with DNA to form alternating stacks of disc bilayered plates and DNA arrays with a repeat distance of 7.5 nm. SAXS and TEM studies revealed that the DNA molecules encapsulated between the disc bilayered plates form ordered arrays with a spacing of around 4–5 nm. The number of stacking layers can be easily tuned from just a few layers to more than one hundred layers by adjusting the doping percentage of the charged lipids. This CB–DNA complex is quite stable against increases in temperature above the chain-melting temperature of the long chain lipids. Due to the flexible size tunability (number of stacking layers) and the unique structure of the packing of the DNA arrays with 50–100 nm size disc bilayered plates, the CB–DNA complexes are promising as novel non-viral vectors for gene delivery.

Received 21st June 2013
Accepted 7th October 2013

DOI: 10.1039/c3sm51703a

www.rsc.org/softmatter

## Introduction

Great efforts have been carried out in the development of DNA–lipid complexes for non-viral gene therapy in recent decades.[1–5] By means of delivering foreign genes into cells, gene therapy promises a cure for many genetic diseases. As an ideal carrier of genes, non-viral vector systems have the advantages of a low cytotoxicity, good immune response and high capability;[5–10] however, the transfection efficiency of non-viral systems is significantly lower than that of viral vectors. There are many studies devoted to the development of stable and effective carriers involving plasmid DNA with polycationic molecules for the delivery of genes into cells.[1,2,6,8,11–14] Previous studies have shown that cationic lipid–DNA (CL–DNA) vectors have potential for promoting the transfection activity. Cationic lipids, such as 1,2-dioleoyl-3-trimethylammonium-propane (DOTAP)[12,15–17] or 3β-[*N*-(*N*′,*N*′-dimethylaminoethane)-carbamoyl]cholesterol (DC-Chol),[2,18–21] are capable of forming large vesicle-based CL–DNA complexes which could approach the anionic cell membrane spontaneously through electrostatic attraction.[12,22,23] At the same time, cationic lipids also serve as protectors to protect plasmid DNA from degradation. Three dimensional CL–DNA complexes in the form of liposomes, called lipoplexes, are typically in the length scale of hundreds of nanometers. Two dimensional DNA arrays are encapsulated between lipid bilayers with a DNA spacing of around 4–5 nm.[12,24] Furthermore, tuning the charged lipid to DNA ratio could vary the DNA spacing and conformational transitions (from $L_\alpha$ to $H_{II}$) could be induced by adding helper lipids, such as the cone shaped DOPE.[13,18,19] Such an inversed CL–DNA structure in a hexagonal packing displays a higher transfection efficiency. The addition of cholesterol to CL–DNA systems has also proved useful in the stabilization of CL–DNA complexes and their resistance to polyanion mediated disassembly.[2,3] The physical and chemical properties of the topological structure are closely correlated to the efficiency of the gene delivery system.[25] The size of CL–DNA complex is also an important factor. For highly efficient gene delivery, the size of the complex should be small enough to facilitate the cellular uptake. It is a critical concern and challenge for researchers to develop small and size-tunable CL–DNA complexes. A typical example is the large cationic PEI–DNA polyplex. Its transfection efficiency is enhanced when the size is decreased from 2000 nm to 100 nm.[5] Therefore, developing compact, stable, small size, and size-tunable CL–DNA complex systems is of great importance. In order to study the cationic liposome–DNA complexes, SAXS (Small-Angle X-Ray Scattering) is a useful tool to observe the intercalation of DNA between the lipid bilayers and also the ordering of the encapsulated DNA.[12]

In this study, we have addressed these issues by developing a new CL–DNA complex by packing DNA with disc-shaped bicelles. Disc-shaped bicelles can be spontaneously formed in aqueous solution by mixing long chain lipids with short chain lipids at suitable ratios.[26–28] Disc-shaped bicelles have been

[a]*Department of Engineering and System Science, National Tsing Hua University, Hsinchu, Taiwan, R.O.C. E-mail: tllin@mx.nthu.edu.tw; Fax: +886-3-5728445; Tel: +886-3-5742671*

[b]*National Synchrotron Radiation Research Canter (NSRRC), Hsinchu, Taiwan, R.O.C.*

† Electronic supplementary information (ESI) available. See DOI: 10.1039/c3sm51703a

Published on 07 October 2013. Downloaded by National Tsing Hua University on 07/11/2013 14:17:47.

widely used as model membrane systems for the investigation of protein–membrane interactions.[29–31] In contrast to the conventional vesicle-based CL–DNA complexes, cationic bicelles can condense DNA into ordered and compact nanostructures of linearly stacked bicelle–DNA complexes. The formation of these alternatively stacked bicelle–DNA complexes is attributed to the electrostatic attraction of cationic bicelles with DNA.[23,32,33] The surface charge density and charge distribution of the cationic lipid bilayer play critical roles in the lipid bilayer–DNA complexation.[22,34–36] In the following sections, we will discuss how the structure of the CB–DNA complex can be tuned by varying the charge density of the cationic bicelles and the DNA concentration. Furthermore, the structural stability of such CB–DNA complexes against temperature variations will also be discussed. The charge density of the disc-shaped bicelles can be controlled by varying the doping amounts of cationic lipids in the DPPC/di$C_7$PC disc bicelles. The structure of the CB–DNA complexes can be tuned by adjusting the doping percentage $\chi$ of the charged lipid and the concentration of DNA. In this study, SAXS and TEM were used in the characterization of the structure of the CB–DNA complexes. The charge ratio of lipid to DNA, as well as the surface charge density (related to the doping percentage), has been reported to affect the structure of CL–DNA significantly.[17,34] However, such CL–DNA charge interaction models can not be directly applied in the case of the CB–DNA systems in which the planar bicelles have a finite size typically smaller than the DNA molecules and can also present edge effects.

## Experimental section

### Materials and sample preparation

The zwitterionic lipids with long chain 1,2-dihexadecanoyl-*sn-glycero*-3-phosphocholine (DPPC) and short chain 1,2-diheptanoyl-*sn-glycero*-3-phosphocholine (di$C_7$PC), and the cationic lipids 3β-[*N*-(*N*′,*N*′-dimethylaminoethane)-carbamoyl] cholesterol hydrochloride (DC-Chol) and 1,2-dioleoyl-3-trimethylammonium-propane (DOTAP) were purchased from Avanti Co. The cationic surfactant hexadecyl-trimethyl-ammonium bromide (CTAB) was purchased from Sigma Co. The type XIV linear DNA from sodium salts of herring testes (Na content 6.2% and $H_2O$ content 4.5%) was purchased from Sigma, and the molecular weights used in the present work were 700 and 2000 base pairs (a base pair has a molecular weight of 649 g mol$^{-1}$ and a distance of 3.4 Å). All chemicals were used without further purification. In this study, the long chain and short chain lipids were used to compose the planar part and rim region of the disc bicelles, respectively, at a molar ratio of 3 to 1.[28,30,37] The total long chain lipid concentration, including DPPC and the cationic lipid, was kept at 10 mM and the short chain lipid (di$C_7$PC) was kept at 3.33 mM. The molar fraction of the cationic lipid in the long chain lipids is denoted by $\chi$. Note that these cationic species are supposed to be located in the planar region of the bicelle and can only slightly affect its disc-shape and size due to differences on the headgroup size. The appropriate amount of lipids was first dissolved in chloroform at the desired molar ratio. The mixture solvents were evaporated and all traces of solvent were then removed entirely in a vacuum oven for at least 8 hours. Subsequently, the dry residue was rehydrated by adding a DNA aqueous solution and treated by bath sonication at a temperature of 30 °C for 5 minutes in order to homogenize the bicelle–DNA suspension in $H_2O$.

### SAXS and TEM

SAXS measurements were carried out in a SAXS beamline 23A at NSRRC, Hsinchu, Taiwan.[38] The photon energy and sample-to-detector distance were set to be 14 keV ($\Delta E/E = 1/7000$) and 2700 mm, respectively, in order to cover a scattering transfer, $Q = (4\pi/\lambda)\sin(\theta/2)$, range from 0.008 to 0.35 Å$^{-1}$. Liquid samples were loaded in a cell with thickness of 5 mm and a Kapton-walled window at 25 °C. Scattered data were collected by means of a 2D MarCCD detector. We performed circular averaging on 2D images to 1D intensity-wave vector functions after the background was subtracted from the data. At the same time, TEM samples were prepared as previously reported.[39,40] Solution samples were first diluted appropriately and dripped onto a copper grid with a supported membrane for 5 minutes. The extra solution was then absorbed with filter paper. In order to enhance the sample contrast, we applied a negative staining with uranyl acetate (1 wt%) for 30 seconds.[41] Our TEM images were taken at 100 kV in a JEOL JEM-1230 at the Chang Gung University, Taiwan.

### Dynamic light scattering (DLS)

The size of the CB–DNA complexes was studied by dynamic light scattering (DLS). A Malvern Zetasizer Nano-ZS was used for the DLS measurements. The sample concentration was kept the same as that for the SAXS measurements. The measured correlation functions were analyzed to obtain the intensity weighted average hydrodynamic radius $R_h$ of the CB–DNA complexes.

## Results and discussion

SAXS has been widely used for studying CL–DNA complex structures and it has revealed that ordered DNA arrays are intercalated between the repeated cationic lipid bilayers of multilamellar liposomes.[12,42] Here, SAXS has also been used to characterize the structure of the CB–DNA complexes as a function of $\chi$ with a constant DNA concentration of 1.07 μM and a total long chain lipid concentration of 10 mM (including the doped cationic lipid) and a short chain lipid concentration of 3.3 mM at 25 °C. The measured SAXS profiles are shown in Fig. 1(A). This CB–DNA system is at the isoelectric point when $\chi = 0.15$ (15% cationic lipids of the total long chain lipids, including the charged lipids) for 1.07 μM anionic DNA with an average of 700 base pairs per DNA molecule. As $\chi$ increases, the scattering profile changes from a discrete bicelle form to multilamellar diffraction patterns. The diffraction peaks become more pronounced as $\chi$ increases. In addition to the growth of the diffraction peaks, the low-$Q$ scattering profiles ($Q < 0.05$ Å$^{-1}$) also change gradually to larger slopes as $\chi$ increases, which also indicates the growth of the aggregates as $\chi$ increases. These are

 This journal is © The Royal Society of Chemistry 2013

Published on 07 October 2013. Downloaded by National Tsing Hua University on 07/11/2013 14:17:47.

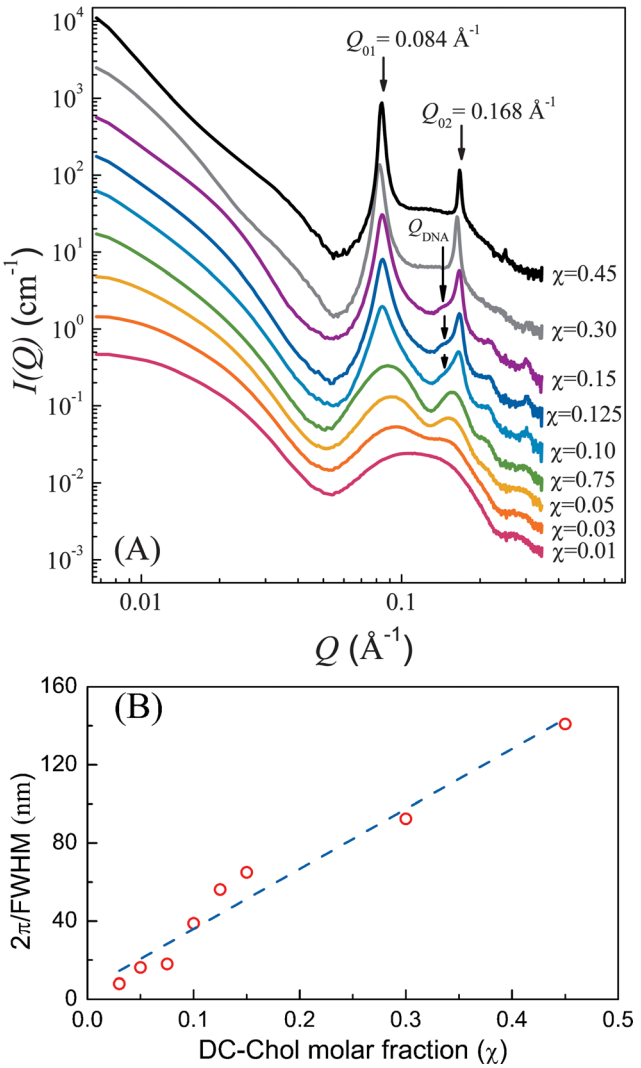


**Fig. 1** (A) The SAXS results of the CB–DNA complexes as a function of $\chi$ with a constant DNA concentration of 1.07 μM at 25 °C. The bicelles are formed with a total long chain lipid concentration of 10 mM (including the doping cationic lipid DC-Chol and DPPC) and a short chain lipid (di$C_7$PC) concentration of 3.3 mM at 25 °C. The molar fraction of the cationic lipid in the long chain lipids is denoted by $\chi$. The arrows at $Q$ = 0.158 Å$^{-1}$ indicate the bump (broad diffraction peak) originated from the DNA arrays encapsulated between disc bicelles. (B) The FWHM, indicative of the stacking degree, of the diffraction peaks located at $Q_{01}$ = 0.084 Å$^{-1}$ as a function of $\chi$.

indicative of the growth of the number of stacked lamellar layers and a growth in size (length). The well-defined 1st and 2nd diffraction peaks, respectively at $Q_{01}$ = 0.084 Å$^{-1}$ and $Q_{02}$ = 0.168 Å$^{-1}$ for $\chi \geq 0.10$, arise from the lamellar structure of the CB–DNA complexes with a periodic spacing of 74.8 Å, as given by $d = 2\pi/Q_{01}$.

The CB–DNA complexes are formed by the intercalation of DNA between cationic bicelles through attractive electrostatic interactions. Without the doping cationic lipids, the bicelles can not form stacked lamellar complexes with DNA. Typical DPPC/di$C_7$PC bicelles have an average diameter of around 19 nm and a thickness of around 4.4 nm in the gel phase as determined by SANS for 20 mM DPPC/5 mM di$C_7$PC bicelles.[26] Therefore, the thickness of the intercalated DNA layer (including the hydrating water), $t_{DNA}$, could be calculated by $t_{DNA} = d - t_{bicelle}$ = 74.8 Å − 44 Å = 30.8 Å, which is close to the typical DNA layer thickness found in CL–DNA systems.[12,43] In addition to the appearance of lamellar diffraction peaks, the diffraction bump (broad diffraction peak) at around $Q_{DNA}$ = 0.158 Å$^{-1}$ that arises from the ordered DNA array intercalated between the bicelles, corresponds to a DNA spacing of $d_{DNA} = 2\pi/Q_{DNA}$ = 39.8 Å. This DNA spacing is comparable to that found in typical CL–DNA systems.[12]

The full width at half maximum (FWHM) of the diffraction peaks can provide information about the correlation length of the ordered structure in the longitudinal stacking direction and the correlation length can act as an indication of the size (length) of the stacked structure. The FWHM of the 1st diffraction peak at $Q_{01}$ = 0.084 Å$^{-1}$ was used to calculate 2π/FWHM as a function of $\chi$, as shown in Fig. 1(B). As mentioned before, the value of 2π/FWHM can be related to the correlation length of the stacked multilayer CB–DNA complex. The correlation length of the stacked multilayer CB–DNA complex varies approximately as a linear function of $\chi$. This means that the size/length of these CB–DNA complexes can be easily tuned by varying the doping percentage of the cationic lipid to adjust the size of CB–DNA from tens to hundreds of nanometers. By increasing the doping percentage of the cationic lipid, the bicelles have a stronger ability to bind DNA and form more stacking layers. The electrostatic interaction gradually overcomes the entropic force to form a larger CB–DNA complex as $\chi$ increases.

The size of the CB–DNA complexes was measured by dynamic light scattering (DLS). Fig. 2 shows the obtained intensity weighted average hydrodynamic radius $R_h$ of the CB–DNA complexes as a function of the molar fraction of the cationic lipid, DC-Chol, in the planar bilayer region. The measured $R_h$ roughly correlates to the doping fraction $\chi$. The dependence of the size on the doping fraction is in accordance with the dependence of the ordering correlation length on $\chi$, as shown in Fig. 2(B). The hydrodynamic radius of CB–DNA increases significantly from 108 nm for $\chi$ = 0.15 to 317 nm for $\chi$ = 0.45. The size polydispersity is around 30%, except in the sample with $\chi$ = 0.45 in which a larger polydispersity of 82% is observed.

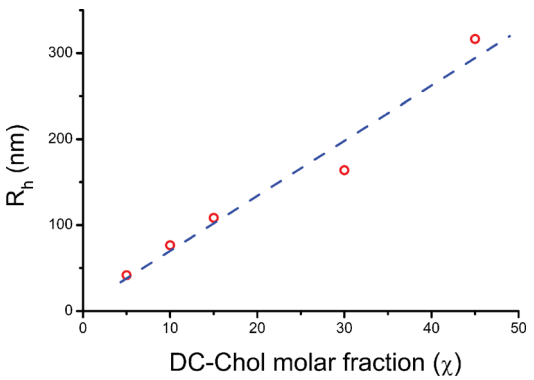


**Fig. 2** The measured hydrodynamic radius of the CB–DNA complexes as a function of $\chi$ with a constant DNA concentration of 1.07 μM at 25 °C. Here, $\chi$ is the molar fraction of the cationic lipid in the long chain lipids.

Published on 07 October 2013. Downloaded by National Tsing Hua University on 07/11/2013 14:17:47.

The hydrodynamic radius is calculated from the apparent diffusion coefficient obtained by DLS. For rigid rodlike particles, the length of the rodlike particle is larger than the value of $2R_h$ and the relationship between the length and the hydrodynamic radius depends on the length to radius ratio. However, in this study, it is found that the length of the CB–DNA complex is comparable to $R_h$. This means that the hydrodynamic radius obtained by DLS for the CB–DNA complex is larger than in a rigid rodlike particle of similar size (same length and same average disc bilayer diameter). This would be a result of the smaller apparent diffusion coefficient of the CB–DNA complex compared to that of a rigid cylinder of the same size. There could be some possible explanations for this difference. For the CB–DNA complex, the average 700 base pair DNA has an average length of 210 nm, which is much larger than the diameter of the disc bilayer, thus some sections of DNA could stick out the disc bilayer into the water phase, which would make the diffusion more difficult (resulting in a smaller diffusion coefficient). Another reason that would also contribute to this difference is the fact that DLS is a scattering intensity weighted average measurement (similar to small-angle scattering), and so it tends to get larger average sizes in a polydisperse system than purely number weighted average size techniques (such as TEM). It can be concluded that both the size ($R_h$) obtained by DLS and the size observed by TEM are comparable and the increase in size correlates well with the increase in the doping charge percentage.

The CB–DNA complex also possesses excellent thermal stability even when the temperature is raised above the chain melting temperature of DPPC (41.5 °C), as investigated by increasing the temperature to 45 °C. Without the complexation with DNA, the bicelles fuse to form large vesicles when the temperature is raised above the chain melting temperature of DPPC.[28,44] As shown in Fig. 3, for the $\chi = 0.15$ sample, the SAXS profile from the CB–DNA complex at 35 °C is almost identical to that at 25 °C except for a slight decrease in the scattering intensity in the low-$Q$ region. Even when the temperature is raised to 45 °C, the CB–DNA complexes still maintain the multi-stacked structure with the same $d$-spacing (same $Q_{01}$ and $Q_{02}$ positions). There is only a slight increase in the FWHM of the diffraction peaks and a slight drop in the low-$Q$ intensity, both indicate that the number of stacking layers has slightly decreased at 45 °C compared to at 25 °C. At higher temperatures, the entropic effects become more important and the size of the aggregates tends to decrease.[28,45] The presence of DNA in the CB–DNA complexes seems to be able to stabilize the bicelle structures even when the temperature is raised above the chain melting temperature of the long chain lipids. The bicelle fusion is suppressed by the formation of the bicelle–DNA stacks. It was also noticed that the diffraction peak originated from the ordered DNA array is no longer visible above 35 °C due to the increased bilayer thermal fluctuations at high temperatures.

The structural stability of such CB–DNA complexes at low pH values, such as at pH 4.5 (in the lysosomes) and 2.8 (in the stomach), was studied by DLS. For $\chi = 0.30$, the measured $R_h$ varied from 328 nm (without pH adjustment) to 294 nm for pH = 4.5 and 281 nm for pH = 2.8. In the case of $\chi = 0.45$, the measured $R_h$ varied from 633 nm (without pH adjustment) to 603 nm for pH = 4.5 and 631 nm for pH = 2.8. It seems that lowering the pH value has no appreciable effect on the size of the CB–DNA complexes. The charge interactions between the cationic bicelles and the DNA are not affected at low pH.

Selected TEM images of the bicelle–DNA complexes are shown in Fig. 4(A)–(G). The 15% DC-Chol doped bicelle is shown in Fig. 4(A). The disc-shaped bicelles, their circular top view and oblate side view, exhibit a narrow size distribution

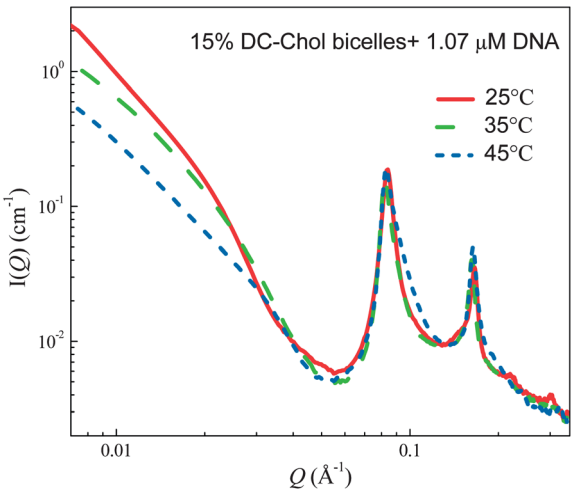


**Fig. 3** The SAXS of 15% DC-Chol CB–DNA complexes at 25 °C (room temperature), 35 °C (close to human temperature and DPPC ripple phase), and 45 °C (over the DPPC melting temperature). The broader lamellar peaks and decreased scattering intensity at the low-$Q$ region indicate a 25% shorter stacking length of the CB–DNA complex.

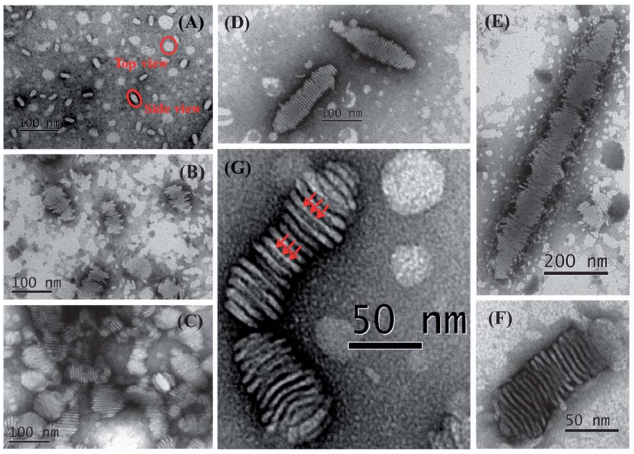


**Fig. 4** The TEM images of (A) 15% DC-Chol bicelles, (B) 15% DC-Chol bicelles with 1.07 μM DNA (700 bp), (C) 15% DC-Chol bicelles with 1.07 μM DNA (2000 bp), (D) 45% DC-Chol bicelles with 1.07 μM DNA, (E) 45% DC-Chol bicelles with 3.21 μM DNA, (F) 15% DOTAP bicelles with 1.07 μM DNA, and (G) 15% CTAB bicelles with 1.07 μM DNA. The arrows in (G) indicate the location of the DNA arrays in between the bicelles. All these TEM samples were diluted from the SAXS samples and measured with negative staining by using 1 wt% uranyl acetate in order to strengthen the contrast between the background and the CB–DNA complexes.


This journal is © The Royal Society of Chemistry 2013

Published on 07 October 2013. Downloaded by National Tsing Hua University on 07/11/2013 14:17:47.

with a diameter of around 20 nm, which is close to the value obtained by the SAXS analysis.[28] The images of 15% DC-Chol bicelle–DNA complexes with 700 bp DNA (~238 nm in length) and 2000 bp DNA are shown in Fig. 4(B) and (C), respectively, where the CB–DNA lamellar complexes that contribute to the diffraction peaks of the SAXS results in Fig. 1 are evident. As shown in Fig. 4(B), the 15% DC-Chol bicelle–700 bp DNA complexes have a width of about 50 nm and a length of about 70–100 nm (about 9–13 layers). The bilayered plates at the ends of these CB–DNA complexes are typically smaller than those in the central region. The typical width of the CB–DNA complexes is about 2.5 times larger than the diameter of a single bicelle. It seems that the bicelles are fused to form larger discs, except at the ends, when they form ordered complexes with DNA. 6–7 disc bicelles would be needed to form the larger disc bilayered plates to build these alternating disc bilayered plate–DNA structures. The typical width of the disc bilayered plates in the CB–DNA complex is around 50 nm, which is comparable to the persistence length of DNA.[46] It is likely that bicelles originally randomly adsorbed on a single DNA molecule start to form an aligned structure and fuse into a larger disc bilayered plate when several DNA molecules with adsorbed bicelles form an ordered array. Such cooperative interactions stabilize the CB–DNA complex. The much smaller bilayered plates at the ends of the CB–DNA complex would not be able to stably adsorb more DNA and would terminate the growth of the CB–DNA complex.

The schematic side view of a CB–DNA complex is depicted in Fig. 5. There could be 6 or slightly more DNA molecules encapsulated between the disc bilayered plates. It is less stable for the side edges of the disc bilayered plate to adsorb DNA. As for the CB–DNA complex formed with 2000 bp DNA, the width of the CB–DNA complex is comparable to that of the 700 bp DNA complex. However, unlike the 700 bp DNA that forms isolated CB–DNA complexes, the 2000 bp DNA forms randomly connected CB–DNA complexes as depicted in Fig. 4(C). The much longer 2000 bp DNA molecules are long enough to stretch further out of the disc bilayered plate and to be shared by another CB–DNA complex in close proximity, such that CB–DNA complexes are connected in different orientations. It is likely that it would take more than one DNA molecule to participate in the linkage of two CB–DNA complexes to form a stable connection. The CB–DNA complex size can be strongly affected by the surface charge density (doping percentage, $\chi$) and DNA concentration. By increasing the doping percentage to 0.45 at a 700 bp DNA concentration of 1.07 μM, as shown in Fig. 4(D), the length of the CB–DNA complexes can reach up to ~200 nm and the width can also reach 100 nm in some regions. Sometimes, branches can also appear. A higher ionic strength helps to stabilize the adsorption by encapsulating longer sections of DNA molecules in larger disc bilayered plates as observed for the complex with $\chi = 0.15$ (see ESI†). Fig. 4(E) shows the result of using a three times higher DNA concentration (3.21 μM) at the same charge doping percentage of 0.45. A higher DNA concentration results in the formation of even longer CB–DNA complexes, of around 900 nm in length, with a slightly larger width of ~100 nm. This shows that the DNA concentration is also important in controlling the size of the CB–DNA complexes.

Besides DC-Chol, other cationic lipids, such as DOTAP and cationic surfactant CTAB, can also be used to form cationic bicelles. The 15% doped DOTAP and CTAB bicelles in complexation with 1.07 μM DNA are, respectively, shown in

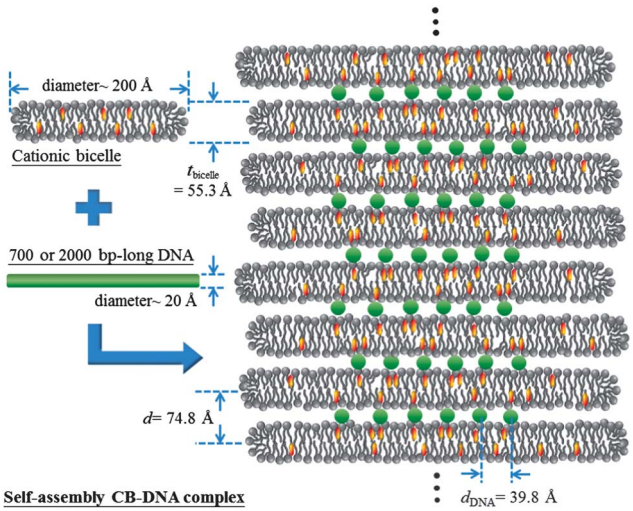


**Fig. 5** Schematic picture of a single cationic bicelle, DNA and the CB–DNA complex. It shows a multilamellar CB–DNA complex formed by mixing cationic bicelles and anionic DNA. The long chain lipid, DPPC, and short chain lipid, $diC_7PC$, form the planar and rim regions, respectively, with the appropriate molar ratio of 3. Doped cationic DC-Chol (denoted in yellow and red, where red indicates the charged head of DC-Chol) was utilized to enhance the charge interactions with the anionic DNA. The side view of the self-assembled CB–DNA complex is shown schematically, where the semiflexible DNA of 700 or 2000 bp is presented as a green rod. We have assumed that the charged species in each bicelle have a uniform distribution in the absence of DNA. After forming the complex with DNA, the charge interactions cause the rearrangement of these charged species. The non-uniform distribution of DC-Chol displaces the DNA rods to the center of the large fused bicelle, and so the DNA induces several bicelles to merge.

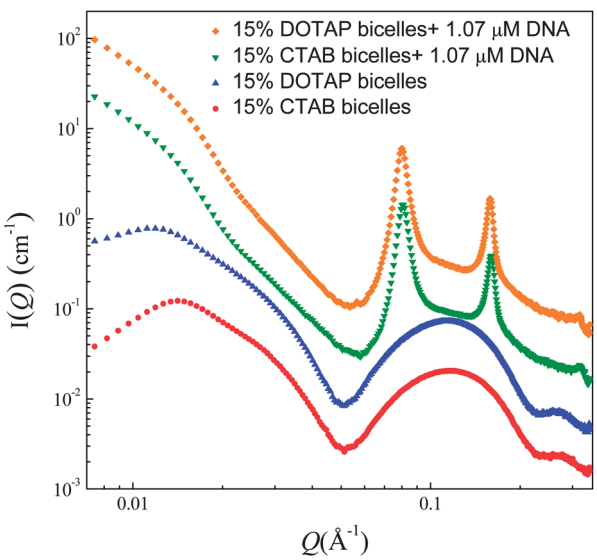


**Fig. 6** The SAXS results of 15% doped cationic DOTAP and CTAB bicelle without and with 1.07 μM DNA. Both DOTAB and CTAB bicelle–DNA complexes show almost the same profile.

Published on 07 October 2013. Downloaded by National Tsing Hua University on 07/11/2013 14:17:47.

Fig. 4(F) and (G). The disc bilayered plates in the DOTAP doped CB–DNA complex have a more uniform size as compared to the quite irregular sizes of the DC-Chol doped disc bilayered plates in their CB–DNA complex. The DNA binding constant of DOTAP is higher than that of DC-Chol,[47] thus DOTAP is expected to exert a stronger binding to DNA even near the side edges of the disc bilayered plates and to form more uniform radial size CB–DNA complexes. As for the 15% CTAB doped CB–DNA complexes, their size and shape are closer to those of 15% doped DC-Chol CB–DNA complexes. The arrows in Fig. 4(G) indicate the location of the DNA encapsulated between the disc bilayered plates with a DNA spacing of ~4 nm, which is consistent with that observed by SAXS (Fig. 1(A)) and other studies.[12] As shown in the ESI† and Fig. 6, the SAXS profiles of the 15% doped DOTAP and CTAB bicelles in complexation with 1.07 μM DNA exhibit a similar scattering pattern as that of the 15% DC-Chol doped CB–DNA complex.

## Conclusions

In summary, cationic lipid or surfactant doped bicelles were found to form novel complex structures with DNA. Disc bilayered plates were formed by fusing bicelles to encapsulate the oppositely charged DNA, which resulted in the formation of alternating bilayered plate–DNA stacking multilayers. The number of stacking layers of the CB–DNA complex can be easily tuned by varying the charge doping percentage to control the size from just a few stacking layers to more than one hundred layers. The size and structure of the lipoplexes are important factors in determining the effectiveness of DNA transfection. The novel CB–DNA complexes developed in this study could be potentially useful in gene delivery and other applications due to the easiness of controlling the complex size, and also due to the relatively small size compared to that of lipoplexes, which have typically sizes larger than 100 nm. In addition to the size tunability, the stacking structure of the CB–DNA complexes could also be beneficial in terms of the interaction with cell membranes and relatively easy DNA release compared to lipoplex systems.

## Acknowledgements

We would like to thank the NSRRC for providing the synchrotron X-ray SAXS beamline 23A and help with the measurements, and the Chang Gung University for the TEM analyses. We would also like to thank Prof. H. C. Chiu for helping with the DLS measurements. This research was supported by the National Science Council, project no. NSC 99-2113-M-007-014-MY3 and NSC 102-2113-M-007 -013 (T.-L. Lin) and the Frontier Research Center on Fundamental and Applied Sciences of Matters of the National Tsing Hua University.

## References

1 P. Scherrer, N. Maurer, M. Monck, E. Saravolac, Y. P. Zhang, J. Wheeler, P. Tam, A. Lam and P. R. Cullis, in *Targeting of Drugs – Strategies for Gene Constructs and Delivery*, ed. G. Gregoriadis and B. McCormack, 2000, vol. 323, pp. 165–185.
2 F. Liu, J. P. Yang, L. Huang and D. X. Liu, *Pharm. Res.*, 1996, **13**, 1856–1860.
3 C. M. Wiethoff and C. R. Middaugh, *J. Pharm. Sci.*, 2003, **92**, 203–217.
4 S. Li and L. Huang, *Gene Ther.*, 2000, **7**, 31–34.
5 M. Thomas and A. M. Klibanov, *Appl. Microbiol. Biotechnol.*, 2003, **62**, 27–34.
6 C. T. de Ilarduya, Y. Sun and N. Duezguenes, *Eur. J. Pharm. Sci.*, 2010, **40**, 159–170.
7 S. Chesnoy and L. Huang, *Annu. Rev. Biophys. Biomol. Struct.*, 2000, **29**, 27–47.
8 M. C. P. de Lima, S. Simoes, P. Pires, H. Faneca and N. Duzgunes, *Adv. Drug Delivery Rev.*, 2001, **47**, 277–294.
9 W. J. Choi, J. K. Kim, S. H. Choi, J. S. Park, W. S. Ahn and C. K. Kim, *Biomaterials*, 2004, **25**, 5893–5903.
10 D. F. Zhi, S. B. Zhang, B. Wang, Y. N. Zhao, B. L. Yang and S. J. Yu, *Bioconjugate Chem.*, 2010, **21**, 563–577.
11 G. C. L. Wong, J. X. Tang, A. Lin, Y. L. Li, P. A. Janmey and C. R. Safinya, *Science*, 2000, **288**, 2035–2039.
12 J. O. Radler, I. Koltover, T. Salditt and C. R. Safinya, *Science*, 1997, **275**, 810–814.
13 I. Koltover, T. Salditt, J. O. Radler and C. R. Safinya, *Science*, 1998, **281**, 78–81.
14 S. Huebner, B. J. Battersby, R. Grimm and G. Cevc, *Biophys. J.*, 1999, **76**, 3158–3166.
15 C. M. Wiethoff, J. G. Koe, G. S. Koe and C. R. Middaugh, *J. Pharm. Sci.*, 2004, **93**, 108–123.
16 K. Crook, B. J. Stevenson, M. Dubouchet and D. J. Porteous, *Gene Ther.*, 1998, **5**, 137–143.
17 D. Hirsch-Lemer and Y. Barenholz, *Biochim. Biophys. Acta, Biomembr.*, 1998, **1370**, 17–30.
18 B. Sternberg, F. L. Sorgi and L. Huang, *FEBS Lett.*, 1994, **356**, 361–366.
19 H. Farhood, N. Serbina and L. Huang, *Biochim. Biophys. Acta, Biomembr.*, 1995, **1235**, 289–295.
20 D. Pozzi, H. Amenitsch, C. Marchini and G. Caracciolo, *Appl. Phys. Lett.*, 2010, **96**, 183703–183703-3.
21 R. G. Cooper, C. J. Etheridge, L. Stewart, J. Marshall, S. Rudginsky, S. H. Cheng and A. D. Miller, *Chem.–Eur. J.*, 1998, **4**, 137–151.
22 J. O. Radler, I. Koltover, A. Jamieson, T. Salditt and C. R. Safinya, *Langmuir*, 1998, **14**, 4272–4283.
23 T. Salditt, I. Koltover, J. O. Radler and C. R. Safinya, *Phys. Rev. E: Stat. Phys., Plasmas, Fluids, Relat. Interdiscip. Top.*, 1998, **58**, 889–904.
24 C. M. Wu, C. Y. Chen, S. Y. Lin and H. L. Chen, *React. Funct. Polym.*, 2011, **71**, 266–271.
25 Y. S. Mel'nikova, S. M. Mel'nikov and J. E. Lofroth, *Biophys. Chem.*, 1999, **81**, 125–141.
26 T. L. Lin, C. C. Liu, M. F. Roberts and S. H. Chen, *J. Phys. Chem.*, 1991, **95**, 6020–6027.
27 M. P. Nieh, C. J. Glinka, S. Krueger, R. S. Prosser and J. Katsaras, *Langmuir*, 2001, **17**, 2629–2638.
28 P. W. Yang, T. L. Lin, Y. Hu and U. S. Jeng, *Chin. J. Phys.*, 2012, **50**, 349–356.

 This journal is © The Royal Society of Chemistry 2013

Published on 07 October 2013. Downloaded by National Tsing Hua University on 07/11/2013 14:17:47.

29 T. Zemb, M. Dubois, B. Deme and T. Gulik-Krzywicki, *Science*, 1999, **283**, 816–819.
30 J. Katsaras, T. A. Harroun, J. Pencer and M. P. Nieh, *Naturwissenschaften*, 2005, **92**, 355–366.
31 A. A. De Angelis, S. C. Howell, A. A. Nevzorov and S. J. Opella, *J. Am. Chem. Soc.*, 2006, **128**, 12256–12267.
32 I. S. Kikuchi and A. M. Carmona-Ribeiro, *J. Phys. Chem. B*, 2000, **104**, 2829–2835.
33 O. Farago, N. Gronbech-Jensen and P. Pincus, *Phys. Rev. Lett.*, 2006, **96**, 018102–018102-4.
34 S. J. Ryhanen, M. J. Saily, T. Paukku, S. Borocci, G. Mancini, J. M. Holopainen and P. K. J. Kinnunen, *Biophys. J.*, 2003, **84**, 578–587.
35 S. J. Ryhanen, J. M. I. Alakoskela and P. K. J. Kinnunen, *Langmuir*, 2005, **21**, 5707–5715.
36 G. Caracciolo, D. Pozzi, A. Amici and H. Amenitsch, *J. Phys. Chem. B*, 2010, **114**, 2028–2032.
37 T. L. Lin, S. H. Chen, N. E. Gabriel and M. F. Roberts, *J. Am. Chem. Soc.*, 1986, **108**, 3499–3507.
38 U-S. Jeng, C. H. Su, C. J. Su, K. F. Liao, W. T. Chuang, Y. H. Lai, J. W. Chang, Y. J. Chen, Y. S. Huang, M. T. Lee, K. L. Yu, J. M. Lin, D. G. Liu, C. F. Chang, C. Y. Liu, C. H. Chang and K. S. Liang, *J. Appl. Crystallogr.*, 2009, **43**, 110–121.
39 N. E. Gabriel and M. F. Roberts, *Biochemistry*, 1986, **25**, 2812–2821.
40 U. L. Khatun, A. Gayen and C. Mukhopadhyay, *Chem. Phys. Lipids*, 2013, **170–171**, 8–18.
41 K. J. Glover, J. A. Whiles, G. H. Wu, N. J. Yu, R. Deems, J. O. Struppe, R. E. Stark, E. A. Komives and R. R. Vold, *Biophys. J.*, 2001, **81**, 2163–2171.
42 A. Rodriguez-Pulido, F. Ortega, O. Llorca, E. Aicart and E. Junquera, *J. Phys. Chem. B*, 2008, **112**, 12555–12565.
43 R. Podgornik, D. C. Rau and V. A. Parsegian, *Macromolecules*, 1989, **22**, 1780–1786.
44 M. E. Ki, G. Riedy, K. H. Langley and M. F. Roberts, *Biochemistry*, 1989, **28**, 8206–8213.
45 T. L. Lin, M. Y. Tseng, S. H. Chen and M. F. Roberts, *J. Phys. Chem.*, 1990, **94**, 7239–7243.
46 S. B. Smith, Y. J. Cui and C. Bustamante, *Science*, 1996, **271**, 795–799.
47 R. Marty, C. N. N'Soukpoe-Kossi, D. M. Charbonneau, L. Kreplak and H. A. Tajmir-Riahi, *Nucleic Acids Res.*, 2009, **37**, 5197–5207.